Polymer Chemistry

PAPER

View Article Online
View Journal | View Issue

Cite this: *Polym. Chem.*, 2014, **5**, 5077

How does a tiny terminal alkynyl end group drive fully hydrophilic homopolymers to self-assemble into multicompartment vesicles and flower-like complex particles?†

Tingting Liu,[a] Wei Tian,*[a] Yunqing Zhu,[b] Yang Bai,[a] Hongxia Yan[a] and Jianzhong Du*[b]

It is a theoretical and technical challenge to construct well-defined nanostructures such as vesicles from fully hydrophilic homopolymers in pure water. In this paper, we incorporate one terminal alkynyl group into a fully hydrophilic linear or non-linear homopolymer to drive its unusual self-assembly in aqueous solution to form multicompartment vesicles, spherical compound micelles, flower-like complex particles, *etc.*, which have been confirmed by transmission electron microscopy (TEM), atomic force microscopy (AFM), dynamic/static light scattering (DLS/SLS) and drug encapsulation experiments. The formation of poly(*N*-isopropyl acrylamide) (NIPAM) and poly[oligo(ethylene glycol) methacrylate] ($POEGMA_{475}$) self-assemblies is mainly determined by the terminal alkynyl group itself (typically 1–3 wt%) while it is independent of other factors such as traditional hydrophobic–hydrophilic balance. Moreover, upon increasing the chain length of PNIPAM homopolymers, multicompartment vesicles, spherical micelles, and large flower-like complex particles can be obtained during the self-assembly process. In contrast, smaller micelles were formed when the kind of terminal alkynyl group attached to the PNIPAM chain was changed from a propargyl isobutyrate group to a (di)propargyl 2-methylpropionamide group. Particularly, a long chain hyperbranched structure with lots of terminal alkynyl groups induces the formation of vesicles. Also, the encapsulation experiment of doxorubicin hydrochloride was employed to further distinguish vesicular and micellar nanostructures. Additionally, the terminal alkynyl group-driven self-assembly has been applied to hydrophilic $POEGMA_{475}$ homopolymers to afford similar nanostructures to PNIPAM homopolymers such as multicompartment vesicles and spherical compound micelles. Our study has opened up a new way to prepare hydrophilic homopolymer self-assemblies with tunable morphology.

Received 10th April 2014
Accepted 3rd May 2014

DOI: 10.1039/c4py00501e

www.rsc.org/polymers

Introduction

Self-assembly of amphiphilic block copolymers (ABCs) can afford a range of nanostructures such as spherical micelles, vesicles, cylinders, fibers, helical superstructures, and macroscopic tubes, which has aroused much attention from materials science to biology.[1–7] However, the strictly distinguishable hydrophobic and hydrophilic segments and the high demands on the synthesis of ABCs have limited their application in the above-mentioned fields. In recent years, amphiphilic homopolymer self-assembly has been investigated aiming to avoid relatively complicated or time-consuming synthetic procedures compared with traditional ABCs.[8–11] Homopolymer assemblies are indeed unique and therefore could find interesting applications in a broad range of areas including dye and drug encapsulation, separation, enzyme inhibition, catalysis, and biosensing.[12–18] Thayumanavan reported[8,12–15,19,20] that such homopolymers were capable of providing both micelle-like and inverse micelle-like assemblies depending on the solvent environment, which is an amplified consequence of the molecular level conformational changes in each monomer unit. Additionally, stable nano-/micro-particles,[11,21–24] hollow spheres,[25,26] and vesicles[27–31] can be easily constructed by the controlled self-assembly of a variety of amphiphilic homopolymers.

Considering more accessible homopolymer alternatives and to avoid organic cosolvents during self-assembly, hydrophilic homopolymers prepared from universal monomers could be more widely used as compared to amphiphilic homopolymers. In general, a suitable hydrophilic–hydrophobic balance in the backbone or side chains of amphiphilic homopolymers is

[a]*The Key Laboratory of Space Applied Physics and Chemistry, Ministry of Education and Shaanxi Key Laboratory of Macromolecular Science and Technology, School of Science, Northwestern Polytechnical University, Xi'an, 710072, P. R. China*

[b]*School of Materials Science and Engineering, Tongji University, 4800 Caoan Road, Shanghai, 201804, China. E-mail: happytw_3000@nwpu.edu.cn; jzdu@tongji.edu.cn*

† Electronic supplementary information (ESI) available: Synthesis, characterization and partial self-assembly results of hydrophilic homopolymers. See DOI: 10.1039/c4py00501e

required to form different nanostructures,[8,13,14,19,20] whereas adjusting the hydrophobic fraction in a fully hydrophilic homopolymer is difficult. Therefore, it is necessary to explore new driving forces for the self-assembly of hydrophilic homopolymers.

Recently, researchers have drawn their attention towards the importance of small changes in chain end chemistry (even a single methyl group) in controlling the solution behaviours of water-soluble polymers.[32,33] In particular, it has been found that different end groups have a pronounced effect on the self-assembly of homopolymers.[10,34–36] For example, Cheng *et al.*[34] reported a polystyrene-(carboxylic acid-functionalized polyhedral oligomeric silsesquioxane) conjugate, which can form micelles, vesicles and wormlike cylinders as a result of the effect of POSS-containing end carboxyl group interactions. Zhou *et al.* found that a novel pH-responsive polymer vesicle could be obtained by the aqueous self-assembly of carboxy-terminated hyperbranched polyesters, which was driven by hydrophobic interactions and hydrogen bonds.[10] Until recently, hydrophilic homopolymers synthesized by a series of new RAFT chain transfer agents containing low molecular weight fraction of hydrophobic end groups could self-assemble into well-defined vesicles and other nanostructures.[35] However, close rigid ring structures such as pyrene or cholesterol as the end groups of hydrophilic homopolymers are prerequisite to drive the formation of those well-defined aggregates. Du and O'Reilly *et al.*[36] recently emphasized on the effect of end groups originated from a commonly utilized RAFT chain transfer agent, *S*′-1-dodecyl-(*S*′)-(α,α′-dimethyl-α′′-acetic acid) trithiocarbonate and its simple derivatives, on the self-assembly of hydrophilic homopolymers for the first time. In that case, both α and ω chain ends are still indispensable for the formation of regular nanostructures.

Compared with the above-mentioned simple linear structure, amphiphilic homopolymers with unique non-linear topologies, such as Y-shaped,[37] cyclic,[38] hyperbranched,[39–41] and dendronized,[42] have exhibited some unusual self-assembly behaviour and interesting applications. Therefore, we intend to introduce a kind of simple and usual end group into hydrophilic linear or non-linear homopolymers to drive their self-assembly in aqueous solution. The formation of self-assemblies is mainly determined by the end group itself while it is independent of the hydrophilic–hydrophobic balance, the special hydrophobic groups, and the end-group weight fraction/position in hydrophilic homopolymers. What is more, to demand the requirements of different fields, we intend to further adjust the morphology of self-assembled nanostructures by simply changing the structural parameters of homopolymers. Based on the above considerations and our previous work on the self-assembly of homopolymers,[31,36,43,44] here we report the self-assembly of hydrophilic linear and long chain hyperbranched homopolymers (LCHBHP) driven by terminal alkynyl groups originated from different atom transfer radical polymerization (ATRP) initiators. The morphologies of nanostructures are regulated by adjusting the chain length or the kind of terminal alkynyl group. Additionally, the encapsulation capacity of homopolymer self-assemblies toward the guest molecule was investigated to further distinguish micelles and vesicles.

Results and discussion

To conveniently induce the self-assembly of hydrophilic homopolymers, propargyl 2-bromoisobutyrate (**I$_1$**), propargyl 2-bromo-2-methylpropionamide (**I$_2$**), and dipropargyl 2-bromo-2-methylpropionamide (**I$_3$**) as simple alkynyl group-containing ATRP initiators were first synthesized by conventional esterification or amidation reaction (Scheme 1). For direct comparison and mechanism analysis of the self-assembly, initiators without alkynyl groups such as ethyl 2-bromoisobutyrate (**I$_4$**) and benzyl 2-bromoisobutyrate (**I$_5$**) were prepared by esterification reaction (Scheme 1). Among these ATRP initiators, the molecular structure of **I$_3$** synthesized in our lab was confirmed by ^{1}H and ^{13}C NMR, FTIR, electrospray ionization mass spectrometry (Fig. S1†), and elemental analysis. Others were prepared according to the literature (**I$_1$**, **I$_2$**, and **I$_5$**)[45–47] or commercially available (**I$_4$**). The characterization data are provided in the ESI.†

With the above functional ATRP initiators, a range of hydrophilic homopolymers based on *N*-isopropyl acrylamide (NIPAM) and oligo(ethylene glycol) methacrylate ($OEGMA_{475}$) were synthesized by ATRP, as shown in Scheme 1. As shown in Table S1,† homopolymers **1–5**, **7**, **8**, and **9–11** were synthesized by the ATRP of NIPAM or $OEGMA_{475}$ with single or double terminal alkynyl groups introduced by **I$_1$–I$_3$**, or without alkynyl groups from **I$_4$** and **I$_5$**. Compared with the above linear homopolymers, LCHBHP **6** was prepared by polymerization of AB_2 macromonomers (**5**′, see Scheme 1), PNIPAM containing an azide group at its one end and two terminal propargyl groups at the other end *via* click reaction, based on the report by Pan *et al.*[48] To obtain **5**′, the terminal bromine group of **5** was substituted by the N_3 group *via* the reaction with sodium azide in DMF. SEC/MALLS study shows that the M_w increases from 4100 for **5**′ (**5**) to 44 300 for **6** (Table S1 and Fig. S2B†), indicating the occurrence of polymerization reaction. Furthermore, LCHBHP **6** possesses an intrinsic viscosity (η_n) of 7.0 and an exponent α of 0.43, implying the compact hyperbranched conformation. The ^{1}H NMR spectra of homopolymers **5**, **5**′, and **6** are shown in Fig. S3.† Compared with **5** and **5**′, the appearance of proton in the triazole ring (about $\delta = 7.96$) confirms the occurrence of click reaction in the hyperbranched polymerization process. The NMR data of other homopolymers are listed in the ESI.† Both NMR and SEC/MALLS confirmed the successful synthesis of hydrophilic homopolymers **1–11**. Additionally, monodispersed peaks were observed for **1–11** based on SEC/MALLS elution curves, indicating their high purity (Fig. S2†). The weight fraction of the hydrophobic end group in the whole hydrophilic homopolymer (HPO/HPI) is summarized in Table S1.† Obviously, the HPO/HPI values of all hydrophilic homopolymers are very low.

With a range of hydrophilic homopolymers with various terminal alkynyl groups in-hand, the self-assembly of these polymers in aqueous solution was carefully examined. Here we first take a series of PNIPAM homopolymers (**1–6**) as typical examples. Self-assembly was easily promoted *via* directly dissolving the homopolymer in water with a concentration of 0.2

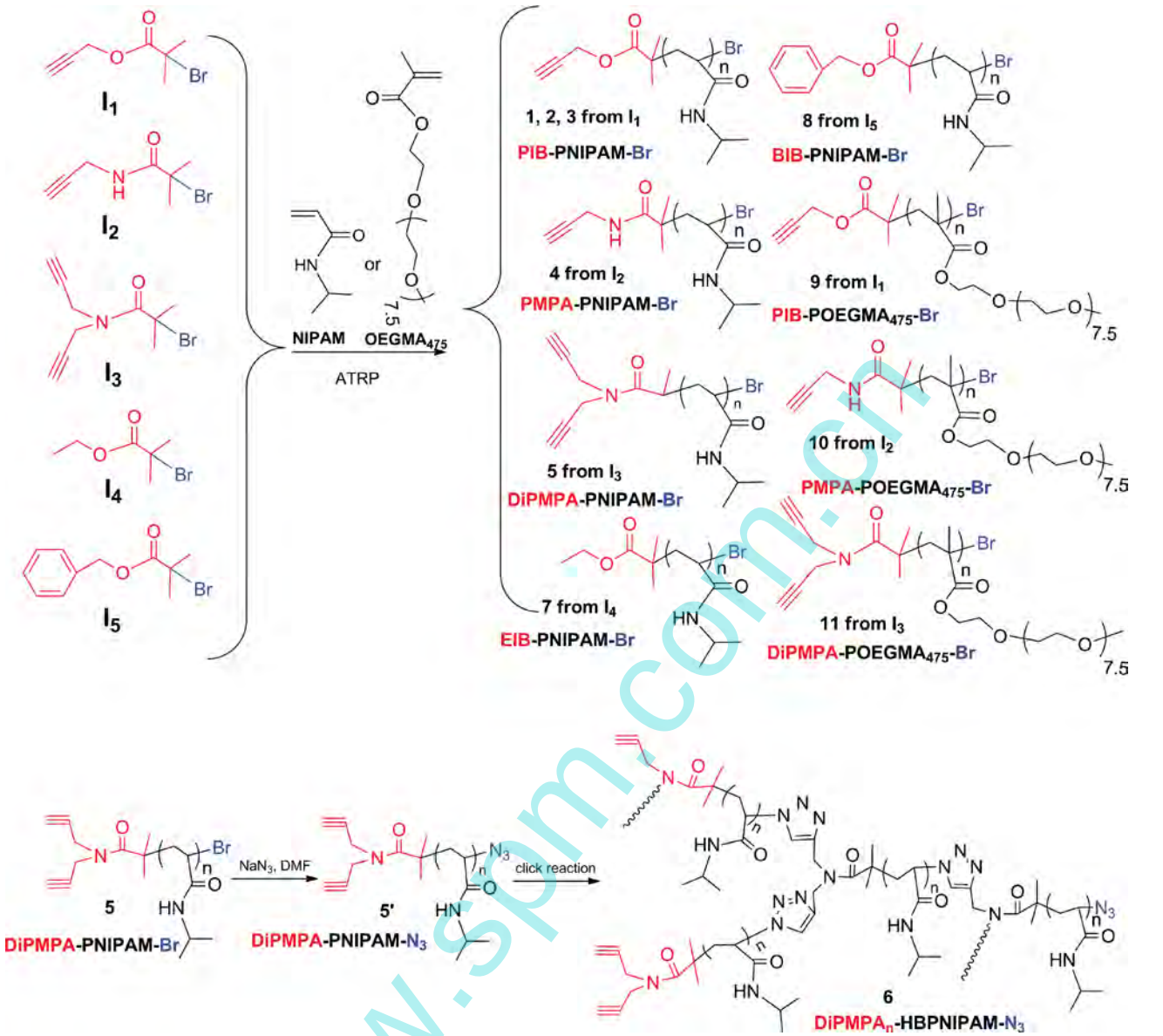

Scheme 1 Molecular structures and synthetic routes for ATRP initiators (I_1–I_5) and homopolymers (**1**–**11**).

mg mL^{-1} at 20 °C. Transmission electron microscopy (TEM), atomic force microscopy (AFM), dynamic/static light scattering (DLS/SLS), fluorescence spectrophotometry (FL) and ^1H NMR (in D_2O) measurements were conducted to obtain deeper insight into the self-assembly morphology and size of these homopolymers.

TEM and AFM were used to image the morphology of self-assemblies from these homopolymers. Typical TEM images were obtained by drying aqueous solutions of samples at room temperature on a copper grid without staining (Fig. 1). Multi-compartment vesicles (MCVs) were suggested by TEM analysis of self-assemblies from homopolymer **1** containing the initiator $\mathbf{I_1}$ group (Fig. 1A and E) with an average diameter (D_{av}) of 89 nm. The MCVs consist of some small compartments (*ca.* 18 nm). While spherical compound micelles (SCMs) with a D_{av} of 183 nm were found in aqueous solution of **2** as shown in Fig. 1B and F. Interestingly, bigger flower-like complex particles (FCPs) with a mean diameter of about 276 nm were observed in aqueous solution of **3** (Fig. 1C and G). Similar morphologies were found in self-assembly of amphiphilic block copolymers,[6,7a] whereas it was observed in fully hydrophilic homopolymer self-assembly for the first time. Furthermore, the morphologies of MCVs, SCMs and FCPs were further confirmed by SLS studies, which will be discussed later.

The evident morphological transformation amongst homopolymers **1**–**3** may be attributed to the different polymer chain lengths. However, compared with the morphology of **1** with a similar polymer chain length, much smaller micelles (*ca.* 27 nm) with less regularity were formed (Fig. S4A and C†) in aqueous solution of homopolymer **4**. Furthermore, the micellar morphology of **5** (*ca.* 25 nm) with a dot-like dark core is more regular than that of **4** as the double terminal alkynyl structure

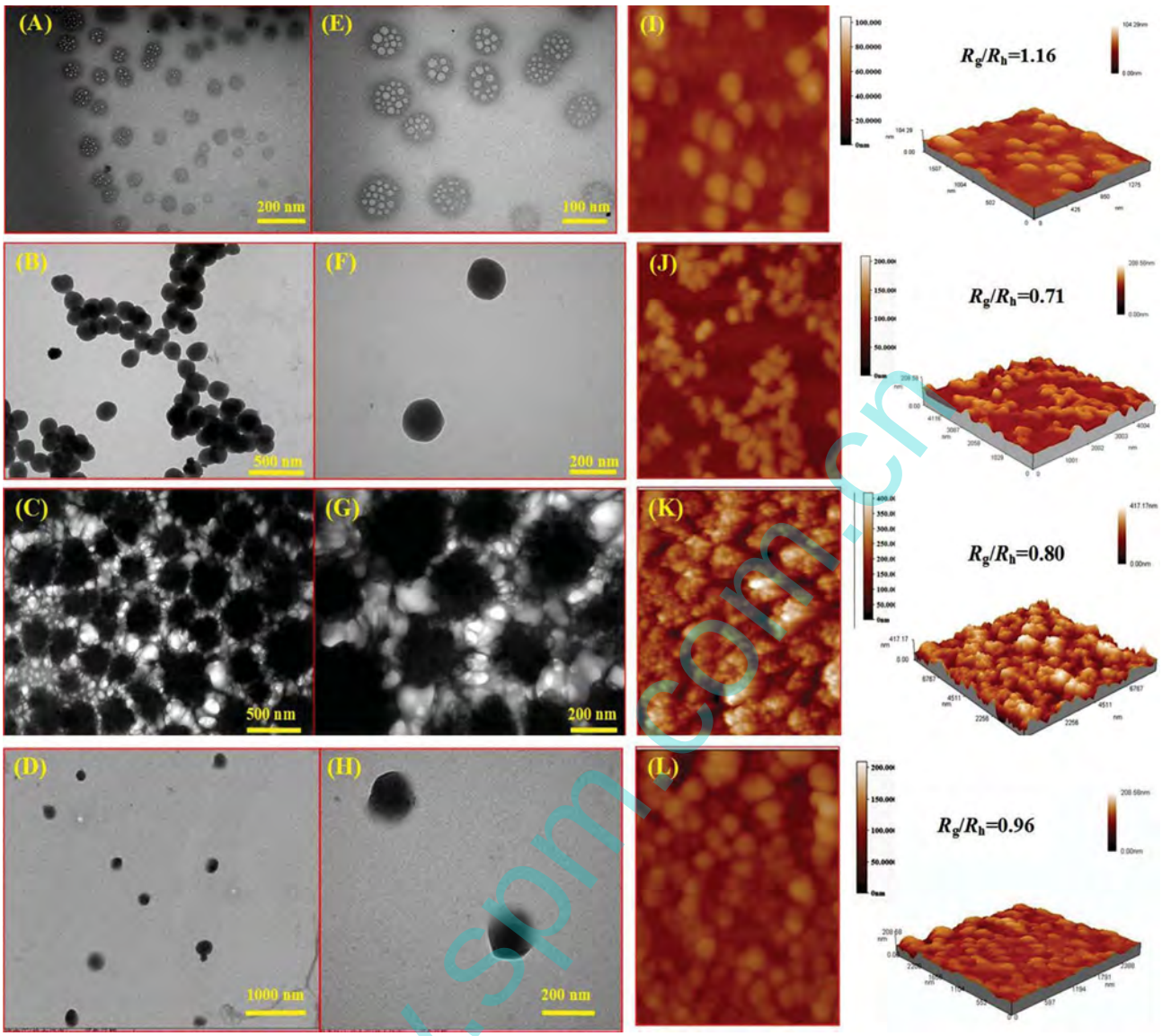

Fig. 1 TEM, AFM and SLS studies of aqueous solutions of homopolymers **1–3** and **6** (A–D for TEM and I–L for AFM) at 0.2 mg mL^{-1} and 20 °C; (E–H) typical magnification images of A–D. The R_g/R_h values were determined by SLS and DLS, which are well consistent with the morphologies revealed by TEM.

was introduced into the homopolymer (Fig. S4B and D†). The change in morphology amongst homopolymers **1**, **4**, and **5** may be induced by the different terminal alkynyl structures originated from initiators $\mathbf{I_1}$, $\mathbf{I_2}$, and $\mathbf{I_3}$, as shown in Scheme 1.

TEM images (Fig. 1D and H) obtained from the aqueous solution of homopolymer **6** with a long hyperbranched chain imply a vesicular structure with a D_{av} value of 181 nm. Similar vesicular morphology was also observed by Wu *et al.* for a dendritic-linear diblock complex.[49] Thus, it seems that the structure of hyperbranched homopolymer **6** is much simpler and the preparation method of directly dissolving the polymer in water is more convenient.

Correspondingly, the AFM images of homopolymers **1–6** were obtained to further verify the formation of the self-assemblies with different morphologies (Fig. 1I–L, S4E and F†), which were generally in agreement with the results of TEM (Fig. 1A–H). The AFM image in Fig. 1I did not show the holes as shown in the TEM images in Fig. 1A and E. This is because the structure of MCVs is similar to a pomegranate, which consists of a smooth and thin shell layer including many small inner cores. The AFM only reveals the surface morphology, rather than the inner structure of MCVs (which can be viewed by TEM). Furthermore, the diameter/height ratios of **1** and **6** are about 10 and 11 respectively, which are much larger than that of **2** (*ca.* 7) with a solid micellar structure, suggesting a vesicular structure. Meantime, AFM results further indicated the capability of controlling the morphologies of self-assemblies of homopolymers **1–6**. The above results confirmed that these PNIPAM homopolymers can indeed self-assemble into nanostructures with different morphologies, which can be well adjusted by simply varying the polymer chain length, the kind of terminal alkynyl group, or the polymer topology, *etc.*

Table 1 Size and morphology of homopolymer self-assemblies in aqueous solution (0.2 mg mL^{-1}) at 20 °C

Code	Sample[a]	Used ATRP initiators	$D_{av,TEM}$[b] (nm)	D_z[c] (nm)	PDI[d]	CMC[e] (mg mL^{-1})	$\mathbf{I_1/I_3}$ above CMC[f]	Morphology
1	PIB-PNIPAM$_{36}$-Br	$\mathbf{I_1}$	89	382	0.287	0.098	1.01	Multicompartment vesicles
2	PIB-PNIPAM$_{45}$-Br	$\mathbf{I_1}$	183	274	0.221	0.051	1.02	Spherical compound micelles
3	PIB-PNIPAM$_{85}$-Br	$\mathbf{I_1}$	276	208	0.223	0.036	0.97	Flower-like complex particles
4	PMPA-PNIPAM$_{38}$-Br	$\mathbf{I_2}$	27	239	0.457	0.001	1.08	Smaller micelles
5	DiPMPA-PNIPAM$_{34}$-Br	$\mathbf{I_3}$	25	169	0.363	0.009	1.04	Smaller micelles
6	DiPMPA$_m$-HBPNIPAM$_{11}$-N$_3$	$\mathbf{I_3}$	181	226	0.234	0.007	1.06	Hollow vesicles
7	EIB-PNIPAM$_{47}$-Br	$\mathbf{I_4}$	—	9	0.594	—	—	—
8	BIB-PNIPAM$_{59}$-Br	$\mathbf{I_5}$	—	13	0.669	—	—	—
9	PIB-P(OEGMA$_{475}$)$_{14}$-Br	$\mathbf{I_1}$	68	328	0.381	0.024	1.09	Multicompartment vesicles and spherical compound micelles
10	PMPA-P(OEGMA$_{475}$)$_{18}$-Br	$\mathbf{I_2}$	184	271	0.323	0.002	1.11	Spherical compound micelles
11	DiPMPA-P(OEGMA$_{475}$)$_{22}$-Br	$\mathbf{I_3}$	126	170	0.283	0.007	1.02	Spherical compound micelles

[a] End groups: see Scheme 1. [b] Average diameter determined by TEM. [c] *Z*-Average diameter determined by DLS. [d] Polydispersity of particles' diameter determined by DLS. [e] The CMC determined by the $\mathbf{I_3/I_1}$ values of pyrene solution with different polymer concentrations (see ESI). [f] The $\mathbf{I_1/I_3}$ value of pure pyrene solution is 1.45.

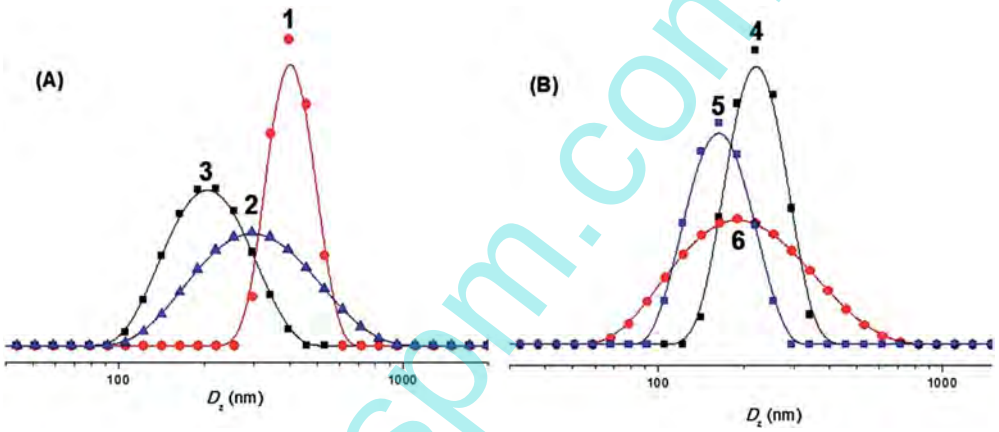

Fig. 2 Typical intensity-averaged diameter distributions of homopolymers **1–3** (A) and **4–6** (B) in aqueous solutions at 0.2 mg mL^{-1} and 20 °C.

The *Z*-average diameter (D_z) and size distribution of self-assemblies of homopolymers **1–6** at a concentration of 0.2 mg mL^{-1} in aqueous solutions were determined by DLS, as shown in Table 1 and Fig. 2A. DLS analysis revealed that the D_z values of **1–3** are 382, 274, and 208, respectively when the degree of polymerization of PNIPAM was increased from 36, 45 to 85. This decrease in size upon increasing the hydrophilic block ratio has been observed in other homopolymer[36] or triblock copolymer[50] systems. Additionally, long chain hyperbranched polymer **6** possesses a bigger size than its linear macromonomer precursor **5** due to its 3D topology structure (Fig. 2B). As shown in Table 1, the D_z values of **1–6** are larger than their $D_{av,TEM}$ values determined from TEM images in Fig. 1. There are two possibilities for this discrepancy. First, TEM and DLS show different morphologies in the solid and swollen states, respectively. Secondly, DLS is much more sensitive to large particles than small particles, whereas both small and large particles can be seen in TEM. To further confirm the observed self-assembly morphologies of these homopolymers, we utilized a combination of SLS and DLS techniques.

The radius of gyration (R_g) is defined as the mass weighted average distance from the center of mass to each mass element, which was measured by monitoring the angular dependence of the sample scattering intensity in SLS, whereas the hydrodynamic radius (R_h) is the representative of the size of a hard sphere that diffuses at the same rate as the particle being measured, which is measured by DLS. Usually, the R_g/R_h value can predict the particle morphology. For example, a solid sphere has an R_g/R_h of 0.774, while a thin-layer hollow sphere of 1.00. Therefore, the R_g/R_h values of homopolymers **1** and **6** are 1.16 and 0.96 indicating vesicular structures (see Fig. 1 as well), whereas those of homopolymers **2–5** are 0.71, 0.80, 0.62, and 0.69, respectively, implying solid structures. Thus, DLS/SLS results further support that homopolymers **1–6** can self-assemble into vesicles or micelles in aqueous solution. Detailed information for R_g/R_h values corresponding to different homopolymer morphologies can be seen in Fig. 1, 7 and S4.†

To further investigate the self-assembly process of homopolymers, the critical aggregation concentration (CAC), which

acts as a key parameter to quantitatively confirm whether the micelles have been formed, was estimated by FL using pyrene as a hydrophobic probe. The ratio of the intensity of the third and first peaks (I_3/I_1) in the emission spectrum is very sensitive to the polarity of the medium surrounding pyrene molecules.[51] Thus, the I_3/I_1 values of the pyrene emission spectra *versus* the logarithm of the polymer concentration are shown in Fig. S5 in the ESI.† The CAC is obtained from the intersection of the baseline and the tangent of the rapidly rising I_3/I_1 curves, indicating the formation of micelles. The CAC values of homopolymers **1–6** listed in Table 1 are higher than those of conventional diblock copolymer systems (*ca.* 0.001–0.003 mg mL^{-1}).[52] The most likely explanation is that an extremely low hydrophobic–hydrophilic balance exists in the structure of these homopolymers. A similar result was found in the study of self-assembly of hydrophilic homopolymers by Du and O'Reilly *et al.*[36] In particular, homopolymers **1–3** containing the I_1 terminal group display a rather high CAC compared to homopolymers **4–6** with the I_2 or I_3 terminal group. However, for the homopolymers carrying the same terminal group (such as **1–3** or **4–6**), the CAC value is relatively close to each other, although **1–3** have different polymer chain lengths, and **4** (or **5**) is a linear homopolymer with only one (or two) terminal group while **6** possesses a long chain hyperbranched structure carrying a large number of terminals. These results indicate that the type of terminal alkynyl group has a more pronounced influence on the self-assembly process of homopolymers compared to other molecular structure parameters. Additionally, the I_1/I_3 values for these polymers above CAC are lower than that of the pure pyrene solution of 1.45, further indicating that a greater amount of pyrene is solubilized in water upon addition of homopolymers. According to the results of Thayumanavan *et al.*,[15,19] the I_1/I_3 value is a measure of the distribution coefficient of pyrene between the bulk solvent and the micellar container. When there is a greater volume of the hydrophobic containers available, the relative I_1/I_3 is likely to be lower.

^{1}H NMR analysis in D_2O was employed to further explore the well-defined structure of self-assemblies. Typical ^{1}H NMR spectra of homopolymers **1** and **4–6** in D_2O are shown in Fig. 3. The disappearance of the proton peak in alkynyl groups (about δ = 2.2–2.3) for **1** and **4–6** suggests that the hydrophobic terminal groups were aggregated together in the polar hydrophilic solution (Fig. 3(A)-a, (B)-a, (C)-a, and (D)-a) compared with the corresponding spectra in DMSO-d_6 (a good solvent for all the building blocks of these homopolymers) (Fig. 3(A)-b, (B)-b, (C)-b and (D)-b). Although hydrogen in the alkynyl group is generally considered as active hydrogen and might be exchanged in D_2O, Fukuzumi *et al.* found that the proton peak of acetylene appears at δ = 2.5 in D_2O.[53] Thus, it is reasonable to confirm the hydrophobic region of self-assemblies by this method. In contrast, proton peaks in the PNIPAM backbone could still be found in both D_2O and DMSO-d_6 (Fig. 3). Based on the above analysis, it is convincing that the terminal alkynyl groups formed the hydrophobic region whereas the PNIPAM chain constructed the hydrophilic outer shell in the self-assembly process of homopolymers **1** and **4–6**. Additionally, the proton in the triazole ring as the branching unit of **6** disappeared in D_2O

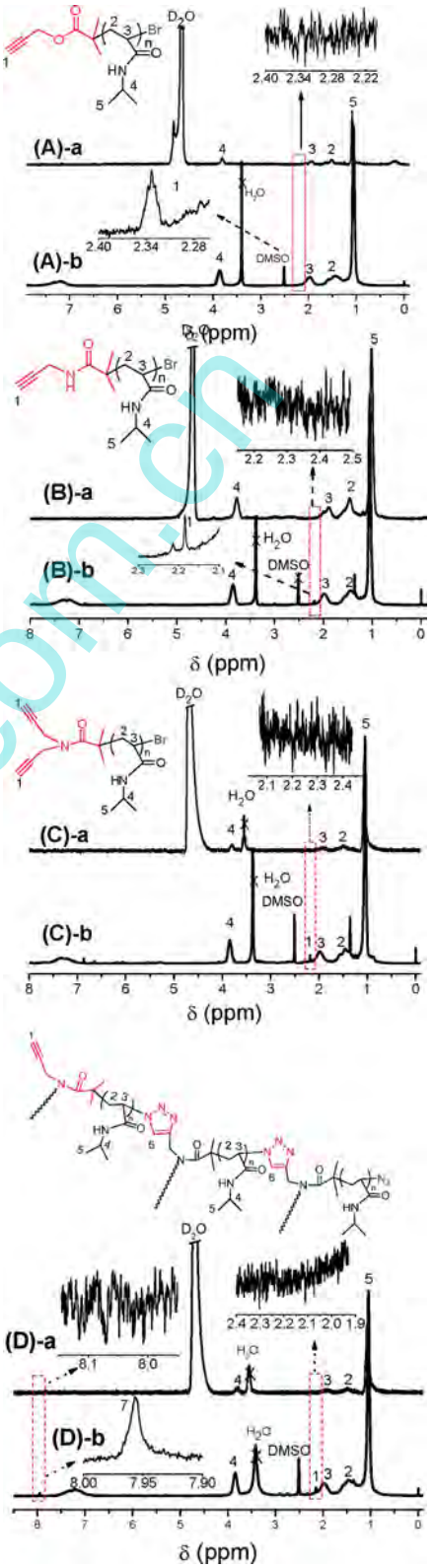

Fig. 3 Typical ^{1}H NMR spectra in D_2O of homopolymers **1** ((A)-a), **4** ((B)-a), **5** ((C)-a), and **6** ((D)-a) with a concentration of 0.2 mg mL^{-1} at 20 °C (^{1}H NMR spectra in DMSO-d_6 of homopolymers **1** ((A)-b), **4** ((B)-b), **5** ((C)-b), and **6** ((D)-b) are shown as controls).

(Fig. 3D-a) compared with its spectrum in DMSO-d_6 (Fig. 3D-b). This result means that the hydrophilic triazole rings were buried in the hydrophobic moieties of vesicles formed by homopolymer **6** (see Fig. 1H).[44]

Based on the above results, we have preliminarily realized that different terminal alkynyl groups as the only hydrophobic component of homopolymers play an important role in their self-assembly behaviours. To further explore the driving force of self-assembly, homopolymers **7** and **8** with ethyl or benzyl group originated from $\mathbf{I_4}$ and $\mathbf{I_5}$ (Scheme 1) were used as controls. No regular morphology can be observed during the TEM analyses of **7** and **8** aqueous solution. Correspondingly, their D_z values are about 10 nm and their PDIs are beyond the reliable value of 0.5 (Table 1 and Fig. S6†). In general, when the D_z value of particles is lower than 10 nm, it is considered as a polymer chain, rather than a self-assembled nanostructure. What is more, with increasing the polymer concentrations of **7** and **8** the $\mathbf{I_3}/\mathbf{I_1}$ values remain nearly unchanged (Fig. S5G and S5H†), indicating the characteristics of pyrene molecules in the aqueous environment while not in the micellar container. According to these results, we can conclude that the self-assembly is not formed for homopolymers **7** and **8** without terminal alkynyl groups. Besides, Du and O'Reilly *et al.* reported that the hydrophilic homopolymer with only one highly hydrophobic end group (such as fluorescent pyrene group) did not self-assemble into regular nanostructures in aqueous solution.[36] This result indicates that the presence of a terminal alkynyl group is demonstrated to be a crucial structural requirement for the formation of hydrophilic homopolymer aggregates. On the other hand, given the extremely low HPO/HPI values of these homopolymers (Table S1†) and the formation of homopolymer aggregates under varied HPO/HPI values, the hydrophilic–hydrophobic balance should not be considered as the key factor for the self-assembly, although the hydrophobic component in general amphiphilic species is primarily responsible for driving self-assembly.[35] This viewpoint can be further confirmed by examining the hydrophilic–hydrophobic transition of homopolymers **1–6** in aqueous solution. Variable temperature UV-vis spectrometry was employed in the present experiments with a constant polymer concentration of 0.2 mg mL^{-1} at a constant heating rate of 1 °C min^{-1}. The transmittance of these homopolymer aqueous solutions decreased with increasing temperature, indicating a hydrophilic–hydrophobic transition, as shown in Fig. S7.† The lower critical solution temperature (LCST) of these homopolymers is evidently higher than that of the temperature of self-assembly occurrence, which is only 20 °C. This result indicates that the hydrophilic–hydrophobic balance is almost impossible to be broken due to the LCST behaviour of PNIPAM as homopolymer self-assemblies were formed in aqueous solution at 20 °C. Additionally, all aqueous solutions of homopolymer self-assemblies are completely transparent and stable. For example, the digital photos of homopolymer **2** solutions at 20 and 70 °C are shown in Fig. 4. Therefore, it is credible that the terminal alkynyl group is the main driving force of self-assembly of hydrophilic homopolymers.

In this paper, the terminal alkynyl group-driven self-assembly is reported for the first time. It seems difficult to

Fig. 4 Digital images of nanostructure solution (A) and phase transition above LCST (B) by direct dissolution of homopolymer **2** in H_2O at 0.2 mg mL^{-1}.

understand the tiny terminal alkynyl group to drive the self-assembly. By comparing with other end groups such as pyrene, cholesteryl, or dodecyl groups, which have been utilized to induce the self-assembly of hydrophilic homopolymers,[35,36] alkynyl as a simple functional group has no strong intermolecular interaction (such as π–π interactions) and high hydrophobicity. In our opinion, active hydrogen existing in unsaturated triple bonding of the alkynyl group may form intermolecular hydrogen bonding with an oxygen atom of the carbonyl group, leading to the formation of different structural aggregates, such as MCVs, SCMs, and FCPs (Scheme 2). To confirm the existence of hydrogen bonding in the self-assembly process, the FTIR-ATR spectra of homopolymers **1–6** in THF and water were compared. Owing to similar spectra and results, we here only take homopolymer **2** as a typical example (see Fig. 5) to discuss the formation of hydrogen bonding while others are shown in Fig. S8.† As shown in Fig. 5, one significant change can be seen in the absorbance peak of C=O groups in homopolymer **2** spectra. Comparing the spectra of homopolymer **2** solution in THF and homopolymer **2** self-assembly, the peaks at about 1648 cm^{-1} are shifted to lower wavenumbers of 1643 cm^{-1}, respectively, along with the expanding and strengthening of C=O absorbance. The formation of strong inter/intra-polymer hydrogen bonding might contribute to the above obvious shifting in the homopolymer **2** spectra. This result is in agreement with a report on the hydrogen bonding-mediated vesicular self-assembly by Ghosh *et al.*[54] It should be noticed that the absorbance peak of the alkynyl group could not be observed in THF and water. This might be attributed to the low end group content and solvent effect. However, the action of intermolecular hydrogen bonding from amino, carboxyl, or hydroxyl group in the self-assembly of homopolymers has been found and further investigated by different research groups.[16,24,31,55]

To examine the encapsulation function of homopolymer self-assemblies, water-soluble doxorubicin hydrochloride (DOX·HCl) was selected as the guest molecule (Scheme S1†) because its main absorption peak can be easily detected by fluorescence emission spectroscopy in an aqueous solution. Fig. 6 shows the fluorescence emission spectra of DOX·HCl solutions in the presence of homopolymers **1** and **4–6**. Fig. 6 presents that the peak intensities of DOX·HCl in homopolymer solutions regularly decrease (0.5 mg mL^{-1} to 2.5 mg mL^{-1}).

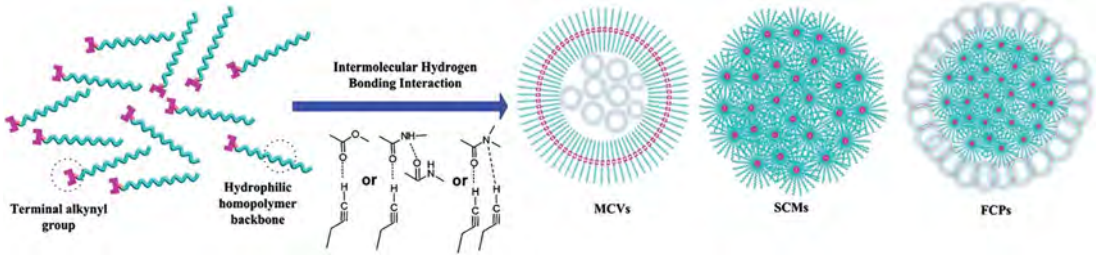

Scheme 2 Schematic representation of the possible self-assembly mechanism of terminal alkynyl group-driven hydrophilic homopolymers.

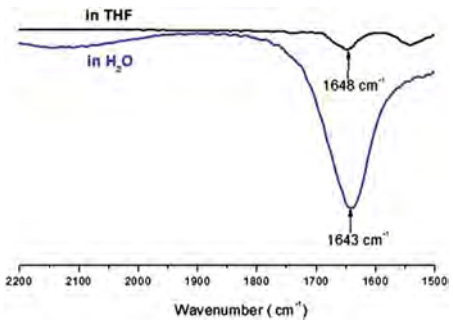

Fig. 5 FTIR-ATR spectra of homopolymer **2** solution in THF and its nanostructure in H_2O at 0.2 mg mL^{-1} and 20 °C.

This phenomenon reveals that DOX·HCl molecules can be encapsulated into the hollow cavity of vesicles or the solid micelle core.[56] However, the peak intensities of DOX·HCl in homopolymer solutions present a more evident decreased tendency in Fig. 6A and D than in Fig. 6B and C, which also indicates the enhanced encapsulation ability of homopolymers **1** and **6** toward DOX·HCl molecules compared with **4** and **5**. Additionally, the inset pictures in Fig. 6 also show that the emission intensities at the λ_{max} value of DOX·HCl decrease with increasing homopolymer concentration. The above results further indicated different self-assembly morphologies of homopolymers **1** and **4–6** in aqueous solution. For **1** and **6** with

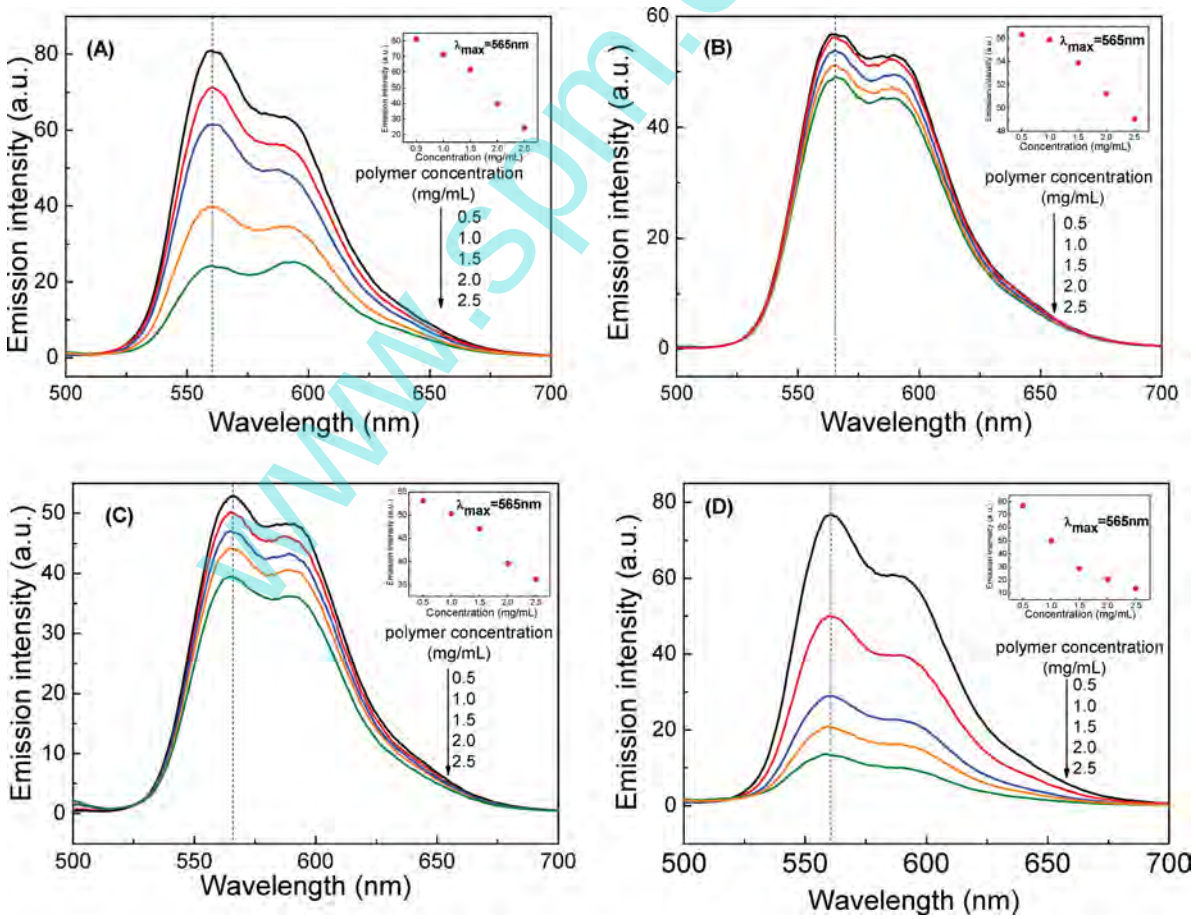

Fig. 6 Fluorescence emission spectra of DOX·HCl aqueous solutions in the presence of different homopolymers with increasing concentration (A, B, C, and D represent homopolymers **1**, **4**, **5**, and **6**, respectively).

hollow morphology (Fig.1E, H, I and L), more encapsulation space can be supplied for hydrophilic DOX·HCl due to the existence of the hollow structure, whereas for **4** and **5** micelles with a small hydrophobic solid micelle core (Fig. 1F and G), it is difficult to encapsulate hydrophilic DOX·HCl molecules. Only a small amount of free hydrophobic DOX can be loaded in the hydrophobic core of micelles. Therefore, the results of the encapsulation experiment are in agreement with TEM, AFM and DLS/SLS results.

Finally, we intend to confirm that the terminal alkynyl group-driven self-assembly can be applied to other hydrophilic homopolymers. For example, the self-assembly of homopolymers **9–11** in aqueous solution was evaluated by TEM, DLS/SLS and FL. Evident vesicular or micellar structures were found in the aqueous solutions of homopolymers **9–11** as shown in Fig. 7. Interestingly, different self-assembly morphologies including MCVs and SCMs coexisted in the self-assembly system of homopolymer **9** (Fig. 7A and A′). The corresponding formation mechanism is still not clear, however, this phenomenon implies that the self-assembly morphology should have a direct correlation with the kind of alkynyl group and polymer chain according to our above analysis. However,

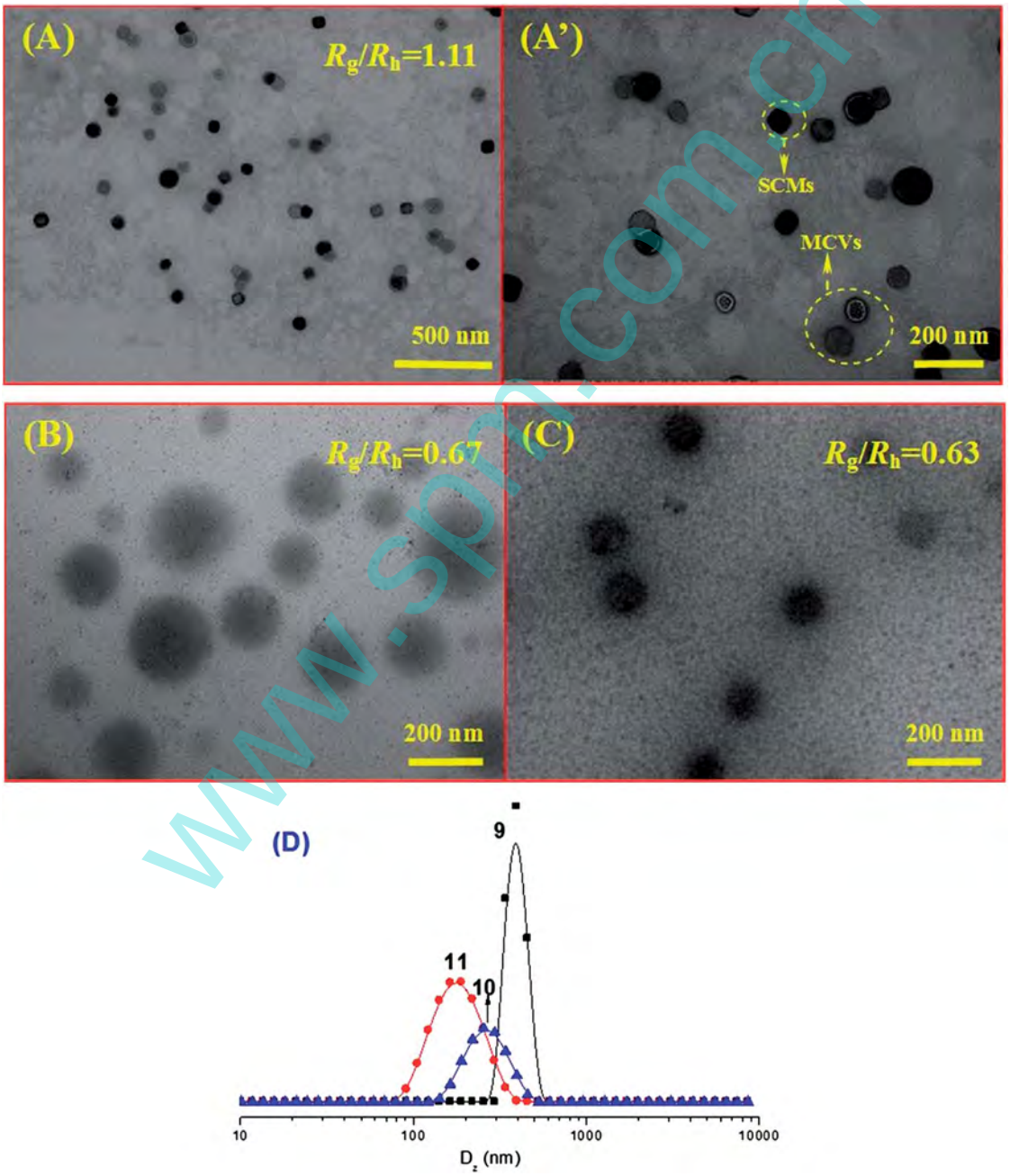

Fig. 7 Transmission electron microscopy (TEM) images, static light scattering (SLS) studies (A–C for **9–11**) and typical intensity diameter distributions (D) of homopolymers **9–11** in aqueous solutions at 0.2 mg mL^{-1} and 20 °C.

MCVs were also found in the aqueous solutions of homopolymer **1**, which possess the same terminal group while different polymer chains with **9**. Additionally, the results of DLS/SLS and CMC of homopolymers **9–11** in aqueous solutions listed in Table 1 and shown in Fig. 7 and S5I–S5K† were in accordance with the results of TEM, further confirming the formation of different self-assemblies. This indicates that different polymer chains may themselves affect the final self-assembly morphology of homopolymers. However, it is definite that the terminal alkynyl group from different ATRP initiators (**I_1–I_3**) is the most crucial factor when considering the self-assembly of hydrophilic homopolymers.

Conclusions

Fully hydrophilic linear or long chain hyperbranched homopolymers with terminal alkynyl groups can be directly dissolved in water to form nanostructures such as multicompartment vesicles, spherical compound micelles, and flower-like complex particles. The terminal alkynyl group is the main driving force of self-assembly of hydrophilic homopolymers. TEM and AFM observations and SLS studies confirmed that PNIPAM homopolymers are able to self-assemble into different nanostructures, such as MCVs, SCMs, FCPs, simple micelles, and simple vesicles, which are closely dependent on the polymer chain length, the kind of terminal alkynyl group, and the polymer topological structure. Furthermore, FL and ^{1}H NMR in D_2O revealed the formation and components of homopolymer self-assemblies. The encapsulation experiment of doxorubicin hydrochloride further distinguishes vesicular and micellar structures. As a result, the terminal alkynyl group-driven self-assembly has been successfully applied to other homopolymers, such as hydrophilic $POEGMA_{475}$ to form vesicles and micelles. Therefore, terminal alkynyl group-driven self-assembly opens up a convenient and effective way to prepare hydrophilic homopolymer-based nanostructures with tunable morphology for potential applications in drug delivery, biosensors, nanoreactors, and enzyme-catalyzed reactions.

Experimental section

Materials

I_4 was purchased from J&K Chemical Technology (China). Tris[2-(dimethylamino)ethyl]amine (Me_6TREN, 99%, Alfa Aesar), ethyl 2-bromoisobutyrate (EBIB, 99%, Alfa Aesar), $OEGMA_{475}$ ($M_n = 475$ g mol^{-1}, 98%, Aldrich), and NIPAM (99%, Acros) were used as received. *N*,*N*,*N*′,*N*″,*N*″-Pentamethyldiethylenetriamine (PMDETA) was supplied by Yutian Chemical, Ltd. (Liyang City, China) and used as received without further purification. 4-Dimethylaminopyridine (DMAP, 95%) was purchased from Sinopharm Chemical Reagent Co., Ltd., Shanghai, China. DOX·HCl was purchased from Alfa Aesar China. CuBr was stirred with acetic acid overnight, then washed with ethanol and dried under vacuum at 25 °C. Other reagents were purchased from Tianjin Kermel Chemical Reagents Development Center (Tianjin City, China). They were dried with 4 Å grade molecular sieves before use without further purification.

Polymer structure characterization

FTIR spectra were obtained on a Nicolet iS10 spectrometer (Nicolet, USA), casting samples into thin films on KBr. Transition mode was used and the wavenumber range was set from 4000 cm^{-1} to 500 cm^{-1}. FTIR-ATR spectra of the homopolymer **1–6** solutions were processed by ATR correction. A solution of the sample in either THF or water was placed in the liquid cell, and the spectra of the solutions were recorded. ^{1}H NMR and ^{13}C NMR spectra were recorded on a Bruker Avance 300 spectrometer (Bruker BioSpin, Switzerland) operating at 300 MHz (^{1}H) in DMSO-d_6 or D_2O. Electrospray ionization mass spectrometry was recorded using a microTOF-QII10280 (Varian Inc., USA). Elemental analysis was conducted on a VARIO ELIII elemental analysis meter (VARIO, Germany). The molecular structure parameters of the resulting polymers were determined on a DAWN EOS SEC/MALLS instrument equipped with a viscometer (Wyatt Technology, USA). HPLC-grade DMF containing LiCl (0.01 mol L^{-1}) (at 40 °C) or THF (at 25 °C) was used as an eluent at a flow rate of 0.5 mL min^{-1}. The chromatographic system consisted of a Waters 515 pump, differential refractometer (Optilab rEX), and one-column MZ 10^3 Å 300 × 8.0 mm for the DMF system as well as two-column MZ 10^3 Å and 10^4 Å for the THF system. The MALLS detector (DAWN EOS), quasi-elastic light scattering (QELS), and differential viscosity meter (ViscoStar) were placed between the SEC and the refractive index detector. The molecular weight (M_w) and molecular weight distribution (MWD) were determined using a SEC/DAWN EOS/OptilabrEX/QELS model. The intrinsic viscosity (η_n) was determined using a SEC/DAWN EOS/OptilabrEX/ViscoStar model. ASTRA software (Version 5.1.3.0) was utilized for acquisition and analysis of data.

Polymer solution characterization

The size and morphology of the unimolecular and multimolecular micelles with different polymer concentrations (2×10^{-2} mg mL^{-1} and 1.5 mg mL^{-1}) were revealed by TEM (Hitachi H-7650, Japan) at an acceleration voltage of 80 kV. Samples were prepared by dropping 10 μL of polymer solution on copper grids without staining and then left to dry in air. The morphology was visualized using AFM with tapping mode and a Nanowizard II controller (Benyuan, CSPM 5500, China). Tip information: radius ≤33 mm, cantilever length 10 μm, width 100 μm, thickness 30 mm, resonant frequency 300 kHz, and force constant 40 N m^{-1}. A Zetasizer Nano-ZS DLS (Malvern Instruments, UK) was used to determine the hydrodynamic diameter of self-assemblies. Each sample was kept at a predetermined temperature for 3 min before measurement without any filter. SLS analysis was performed on a DAWN HELEOS-II multi-angle light scattering detector (Wyatt Technology Corporation, USA) operated at 665 nm, using gallium–arsenic as the incident laser beam source. SLS data were collected at 6 different concentrations of the aggregates and 18 different angles for each concentration. The data were analyzed using the Zimm plot method on HELEOS-II Firmware 2.4.0.4 advanced software to determine R_g.

Polymer solution properties

To obtain the CMC of the polymer solution, the solid polymer was initially dissolved in water with certain pyrene content. Then, the polymer solution was diluted step-by-step to various desired concentrations (from 1×10^{-6} mg mL^{-1} to 0.4 mg mL^{-1}) while keeping the pyrene concentration at around 6×10^{-6} mol L^{-1}. The emission spectra were recorded by FL (Hitachi F-4600, Japan) from 355 nm to 550 nm with an excitation wavelength of 335 nm, and then the $\mathbf{I_3/I_1}$ ratio values of all spectra were calculated.

LCSTs of the homopolymers **1–6** were first determined by UV-vis (Shimadzu UV-2550 model, Japan). Optical transmittances of the homopolymer aqueous solutions with a constant polymer concentration of 0.2 mg mL^{-1} were recorded at 550 nm under different temperature conditions. Sample cells were thermostatted with an external constant temperature controller. The temperature ramp was set at 1 °C min^{-1}. The LCST values of the homopolymers were defined as the temperatures corresponding to 90% transmittance of the aqueous solution during the heating process.[34]

Guest encapsulation of homopolymers **1** and **4–6** was investigated by FL (Hitachi F-4600, Japan) using DOX·HCl (5×10^{-5} mol L^{-1}) as the guest molecule in a buffer solution with ionic strength equal to 0.1 mol L^{-1}. Typically, the homopolymer solution was diluted step-by-step to various desired concentrations (from 0.5 mg mL^{-1} to 2.5 mg mL^{-1}) using different guest molecule solutions. All solutions were maintained for more than 12 h to ensure the binding equilibrium and then stirred prior to measurement.

Acknowledgements

The authors are grateful to the National Natural Science Foundation of China (no. 21374088, 21004049, 21074095, 21174107, and 21374080) and the Program for New Century Excellent Talents of Ministry of Education (NCET-10-0627 and NCET-13-0476) for financial support. W.T. acknowledges the Program of Youth Science and Technology Nova of Shaanxi Province of China (2013KJXX-21), and the Program of New Staff and Research Area Project of NPU (13GH014602). J.D. appreciates the financial support from the Eastern Scholar professorship and Shanghai 1000 plan professorship.

Notes and references

1 L. Zhang and A. Eisenberg, *Science*, 1995, **268**, 1728.
2 J. D. Hartgerink, E. Beniash and S. I. Stupp, *Science*, 2001, **294**, 1684.
3 B. J. Reynwar, G. Illya, V. A. Harmandaris, M. M. Mueller, K. Kremer and M. Deserno, *Nature*, 2007, **447**, 461.
4 A. H. Gröschel, A. Walther, T. I. Löbling, F. H. Schacher, T. Schmalz and A. H. E. Müller, *Nature*, 2013, **503**, 247.
5 (*a*) D. Yan, Y. Zhou and J. Hou, *Science*, 2004, **303**, 65; (*b*) J. Wang, Y. Yao, B. Ji, W. Huang, Y. Zhou and D. Yan, *Chin. J. Polym. Sci.*, 2013, **31**, 218.
6 Y. Chen and J. Du, *Angew. Chem., Int. Ed.*, 2004, **43**, 5084.
7 (*a*) X. Hu, J. Hu, J. Tian, Z. Ge, G. Zhang, K. Luo and S. Liu, *J. Am. Chem. Soc.*, 2013, **135**, 17617; (*b*) J. Rao, Y. Zhang, J. Zhang and S. Liu, *Biomacromolecules*, 2008, **9**, 2586; (*c*) J. Hu and S. Liu, *Macromolecules*, 2010, **43**, 8315; (*d*) Z. Ge, J. Hu, F. Huang and S. Liu, *Angew. Chem., Int. Ed.*, 2009, **48**, 1798; (*e*) Z. Ge, Y. Zhou, J. Xu, H. Liu, D. Chen and S. Liu, *J. Am. Chem. Soc.*, 2009, **131**, 1628.
8 S. Basu, D. Vutukuri, S. Shyamroy, B. Sandanaraj and S. Thayumanavan, *J. Am. Chem. Soc.*, 2004, **126**, 9890.
9 J. N. Cha, H. Birkedal, L. E. Euliss, M. H. Bartl, M. S. Wong, T. J. Deming and G. D. Stucky, *J. Am. Chem. Soc.*, 2003, **125**, 8285.
10 Z. Shi, Y. Zhou and D. Yan, *Macromol. Rapid Commun.*, 2008, **29**, 412.
11 X. Zhou, X. Li, T. Mao, J. Zhang and X. Li, *Soft Matter*, 2011, **7**, 6264.
12 B. S. Sandanaraj, J. Simard, D. R. Vutukuri, R. Hong, V. M. Rotello and S. Thayumanavan, *J. Am. Chem. Soc.*, 2005, **127**, 10693.
13 S. Arumugam, D. R. Vutukuri, S. Thayumanavan and V. Ramamurthy, *J. Am. Chem. Soc.*, 2005, **127**, 13200.
14 S. Basu, D. R. Vutukuri and S. Thayumanavan, *J. Am. Chem. Soc.*, 2005, **127**, 16794.
15 T. S. Kale, A. Klaikherd, B. Popere and S. Thayumanavan, *Langmuir*, 2009, **25**, 9660.
16 B. Li, K. K. L. Cheuk, D. Yang, J. W. Y. Lam, L. Wan, C. Bai and B. Tang, *Macromolecules*, 2003, **36**, 5447.
17 K. S. Sharma, G. Durand, F. Gabel, P. Bazzacco, C. L. Bon, E. Billon-Denis, L. J. Catoire, J. L. Popot, C. Ebel and B. Pucci, *Langmuir*, 2012, **28**, 4625.
18 K. Dan and S. Ghosh, *Macromol. Rapid Commun.*, 2012, **33**, 127.
19 E. N. Savariar, S. V. Aathimanikandan and S. Thayumanavan, *J. Am. Chem. Soc.*, 2006, **128**, 16224.
20 B. S. Sandanaraj, D. Robert and S. Thayumanavan, *J. Am. Chem. Soc.*, 2007, **129**, 3506.
21 J. Cha, H. Birkedal, L. E. Euliss, M. H. Bartl, M. S. Wong, T. J. Deming and G. D. Stucky, *J. Am. Chem. Soc.*, 2003, **125**, 8285.
22 M. Sedlák and C. Koňák, *Macromolecules*, 2009, **42**, 7430.
23 M. Sedlák, C. Koňák and J. Dybal, *Macromolecules*, 2009, **42**, 7439.
24 M. Sedlák, *J. Phys. Chem. B*, 2012, **116**, 2356.
25 N. Li, G. Ye, Y. He and X. Wang, *Chem. Commun.*, 2011, **47**, 4757.
26 M. Changez, N. G. Kang and J. S. Lee, *Small*, 2012, **8**, 1173.
27 Z. Hordyjewicz-Baran, L. C. You, B. Smarsly, R. Sigel and H. Schlaad, *Macromolecules*, 2007, **40**, 3901.
28 M. Changez, N. G. Kang, C. H. Lee and J. S. Lee, *Small*, 2010, **6**, 63.
29 S. R. Mane, V. N. Rao and R. Shunmugam, *ACS Macro Lett.*, 2012, **1**, 482.
30 S. R. Mane, V. N. Rao, K. Chaterjee, H. Dinda, S. Nag, A. Kishore, J. Das Sarma and R. Shunmugam, *Macromolecules*, 2012, **45**, 8037.
31 (*a*) Y. Q. Zhu, L. Liu and J. Z. Du, *Macromolecules*, 2013, **46**, 194; (*b*) Y. Q. Zhu, L. Fan, B. Yang and J. Z. Du, *ACS Nano*, 2014, **8**, 5022.

32 S. Jana, S. P. Rannard and A. I. Cooper, *Chem. Commun.*, 2007, 2962.
33 M. Long, D. W. Thornthwaite, S. H. Rogers, F. R. Livens and S. P. Rannard, *Polym. Chem.*, 2012, **3**, 154.
34 X. Yu, S. Zhong, X. Li, Y. Tu, S. Yang, R. M. V. Horn, C. Ni, D. J. Pochan, R. P. Quirk, C. Wesdemiotis, W. Zhang and S. Z. D. Cheng, *J. Am. Chem. Soc.*, 2010, **132**, 16741.
35 J. Xu, L. Tao, C. Boyer, A. B. Lowe and T. P. Davis, *Macromolecules*, 2011, **44**, 299.
36 J. Du, H. Willcock, J. P. Patterson, I. Portman and R. K. O'Reilly, *Small*, 2011, **7**, 2070.
37 J. P. Patterson, P. Cotanda, E. G. Kelley, A. O. Moughton, A. Lu, T. H. Epps and R. K. O'Reilly, *Polym. Chem.*, 2013, **4**, 2033.
38 B. A. Laurent and S. M. Grayson, *Polym. Chem.*, 2012, **3**, 1846.
39 J. Liu, W. Huang, Y. Pang, P. Huang, X. Zhu, Y. Zhou and D. Yan, *Angew. Chem., Int. Ed.*, 2011, **50**, 9162.
40 J. Liu, Y. Pang, J. Chen, P. Huang, W. Huang, X. Zhu and D. Yan, *Biomaterials*, 2012, **33**, 7765.
41 Y. Jin, L. Song, D. Wang, F. Qiu, D. Yan, B. Zhu and X. Zhu, *Soft Matter*, 2012, **8**, 10017.
42 W. Li and A. Zhang, *Sci. China: Chem.*, 2010, **53**, 2509.
43 L. Fan, H. Lu, K. Zou, J. Chen and J. Du, *Chem. Commun.*, 2013, **49**, 11521.
44 C. Zhou, M. Wang, K. Zou, J. Chen, Y. Zhu and J. Du, *ACS Macro Lett.*, 2013, **2**, 1021.
45 N. V. Tsarevsky, B. S. Sumerlin and K. Matyjaszewski, *Macromolecules*, 2005, **38**, 3558.
46 J. Song, E. Lee and B. K. Cho, *J. Polym. Sci., Part A: Polym. Chem.*, 2013, **51**, 446.
47 N. J. Hovestad, G. V. Koten, S. A. F. Bon and D. M. Haddleton, *Macromolecules*, 2000, **33**, 4048.
48 L. Kong, M. Sun, H. Qiao and C. Pan, *J. Polym. Sci., Part A: Polym. Chem.*, 2010, **48**, 454.
49 Q. Liu, H. Zhang, S. Yin, L. Wu, C. Shao and Z. Su, *Polymer*, 2007, **48**, 3759.
50 A. M. Bivigou-Koumba, E. Gornitz, A. Laschewsky, P. Muller-Buschbaum and C. M. Papadakis, *Colloid Polym. Sci.*, 2010, **288**, 499.
51 I. Astafieva, X. Zhong and A. Eisenberg, *Macromolecules*, 1993, **26**, 7339.
52 M. Wilhelm, C. Zhao, Y. Wang, R. Xu and M. A. Winnik, *Macromolecules*, 1991, **24**, 1033.
53 T. Tachiyama, M. Yoshida, T. Aoyagi and S. Fukuzumi, *Appl. Organomet. Chem.*, 2008, **22**, 205.
54 M. R. Molla and S. Ghosh, *Chem.–Eur. J.*, 2012, **18**, 9860.
55 H. W. Duan, D. Y. Chen, M. Jiang, W. J. Gan, S. J. Li, M. Wang and J. Gong, *J. Am. Chem. Soc.*, 2001, **123**, 12097.
56 (*a*) W. Tian, A. Lv, Y. Xie, X. Wei, B. Liu and X. Lv, *RSC Adv.*, 2012, **2**, 11976–11987; (*b*) W. Tian, X. Fan, T. Liu, Y. Liu, L. Sun, M. Jiang and Y. Huang, *Chem. J. Chin. Univ.*, 2009, **30**, 632–637.